ORIGINAL ARTICLE
https://doi.org/10.5653/cerm.2023.06695
pISSN 2233-8233 · eISSN 2233-8241
Clin Exp Reprod Med [Epub ahead of print]

Protective effect of platelet-rich plasma against structural and functional changes of the adult rat testis in carbimazole-induced hypothyroidism

Hossein Bordbar[1,2], Masoud Sattar-Shamsabadi[1,2], Farzaneh Dehghani[1,2], Fatemeh Karimi[1,2]

[1]Histomorphometry and Stereology Research Center, Shiraz University of Medical Sciences, Shiraz; [2]Department of Anatomy, School of Medicine, Shiraz University of Medical Sciences, Shiraz, Iran

Objective: Hypothyroidism (HT) influences spermatogenesis and is associated with male infertility. Platelet-rich plasma (PRP), a biological product rich in growth factors, promotes tissue repair. In this study, the likely protective effects of PRP on testicular tissue damage in carbimazole (CBZ)-induced HT were evaluated.
Methods: Forty male rats were divided into four groups. HT was induced by administering CBZ (1.35 mg/kg orally, for 45 days). Two doses of PRP (40 μL each, locally injected into the testis on days 15 and 30) were also given. After 45 days, blood samples were taken from the heart to measure triiodothyronine (T3), thyroxine (T4), and testosterone levels, and semen analysis was performed. For stereological assessment, the left testis was removed, fixed, embedded, sectioned, and stained with hematoxylin and eosin. The right testis was excised to evaluate antioxidant levels.
Results: CBZ was demonstrated to induce HT, characterized by significant reductions in T3 and T4. HT was associated with decreased testicular weight, impaired sperm parameters, reduced testosterone concentration, diminished antioxidant activity, reduced volumes of testicular components, and lower total numbers of testicular cells of various types. When HT samples were treated with PRP, improvement was observed for all of these changes. This protective effect could be attributed to the growth factors present in PRP.
Conclusion: PRP appears to prevent the structural changes in the testes and the deterioration in sperm quality caused by CBZ-induced HT. This protective effect is likely due to mitigation of oxidative damage and elevation of testosterone levels.

Keywords: Hypothyroidism; Infertility, male; Platelet-rich plasma; Rats; Testis

Introduction

Male infertility problems include testicular insufficiency, age-related semen deterioration, and exposure to endocrine disruptors [1]. Thyroid disorders, such as Hashimoto thyroiditis, thyroid cancer, and imbalances in thyroid hormones, are also contributing factors to male infertility [2,3]. Previous research has shown that alterations in thyroid hormone levels coincide with changes in reproductive function [4,5]. Thyroid hormones, including triiodothyronine (T3) and thyroxine (T4), play pivotal roles in metabolism, the immune system, and the growth and development of the testes by influencing the hypothalamic-pituitary-testicular axis [2,6]. Hypothyroidism (HT) is a condition resulting from damage to, removal of, or functional inhibition of the thyroid gland [7]. Evidence suggests that HT can result in widespread cellular and organ damage, with the brain, skeletal system, and testicles impacted particularly heavily [8]. Individuals with HT experience a significant decrease in serum testosterone levels, cessation of ejaculation, and a reduction in sexual activity [9]. Moreover, HT adversely influences human spermatogenesis and notice-

Received: November 14, 2023 · Revised: December 26, 2023 · Accepted: January 10, 2024
Corresponding author: **Fatemeh Karimi**
Department of Anatomy, School of Medicine, Shiraz University of Medical Sciences, Shiraz 71348-45794, Iran
Tel: +98-713-2304372 Fax: +98-713-2304372 E-mail: karimi_fa@sums.ac.ir

* This work received financial support from Grant No. 1400-23804, provided by Shiraz University of Medical Sciences, Shiraz, Iran, and was conducted at the Histomorphometry and Stereology Research Center of the same institution.

ably alters sperm morphology. It also impairs sperm parameters, such as sperm count and motility [10]. Sperm abnormalities associated with HT may be due to increased oxidative stress, lipid peroxidation, and compromised antioxidant defense mechanisms, with reactive oxygen species arising from both heightened free radical production and diminished antioxidative capacity [11,12]. Conversely, the potential of treating infertility with growth factors has been recently explored [13]. Platelet-rich plasma (PRP) is a biologically conditioned plasma rich in growth factors, including platelet-derived growth factor (PDGF) and vascular endothelial growth factor (VEGF) [14]. Several studies have examined the effects of PRP on infertility. Dehghani et al. [13] reported beneficial effects of intratesticular PRP injection on atrophic testicular tissue, while Sekerci et al. [15] described positive impacts of PRP on testicular torsion. Consequently, PRP is a promising therapeutic option due to its efficacy and safety, warranting further investigation into its biological impact on sperm quality [16,17]. In this study, we used carbimazole (CBZ), an oral anti-thyroid drug, to experimentally induce HT [18]. Drawing on this background, the present study was designed to examine the potential protective effects of PRP on hormonal measurements, sperm parameters, and testicular tissue changes using stereological assessment, in the context of the detrimental impacts of CBZ-induced HT.

Methods

1. Animals

A total of 40 male Sprague-Dawley rats, aged 8 weeks and weighing 180 to 230 g, were purchased from the Animal Laboratory Center of Shiraz University of Medical Sciences. The rats were maintained on a 12-hour light/12-hour dark cycle and given unlimited access to standard food and water. Animals were housed at room temperature (22±2 °C), with normal humidity. All animal procedures were conducted in accordance with the guidelines established by the Animal Care and Regional Ethics Committee of Shiraz University of Medical Sciences (IR.SUMS.REC.1400.006).

2. Experimental design

The animals were randomized into four groups (n=10 each). The control group received 2 mL of distilled water orally per day for 45 days, along with a 40-μL NaCl solution administered in two doses directly injected into the testes on days 15 and 30. Another group was treated with CBZ at a dose of 1.35 mg/kg, dissolved in 2 mL of distilled water and given orally each day for 45 days [18]. A third group received a combination of CBZ and PRP, with the CBZ administered as in group 2 and the PRP in two 40-μL doses, injected directly into the testes on days 15 and 30 [13]. The fourth group was administered PRP alone, provided in the same fashion as in the group receiving CBZ and PRP. On day 46 of the experiment, all animals were weighed and then sacrificed (Figure 1).

3. PRP preparation

PRP was obtained from 10 adult male Sprague-Dawley rats. Under anesthesia, blood samples were collected from the right ventricle and transferred into test tubes containing 3.2% sodium citrate (Merck) at a 9:1 blood-to-citrate ratio. The preparation involved two centrifugation steps. During the first centrifugation, conducted at 380 ×g for 15 minutes at room temperature, the whole blood was separated into three layers. These included an upper layer, predominantly consisting of platelets and white blood cells (WBCs); a thin middle layer (known as the buffy coat) that is rich in WBCs; and a bottom layer, mainly composed of red blood cells (RBCs). The majority of the RBCs were discarded, and the upper layer and buffy coat were transferred to a sterile tube and centrifuged at 1,300 ×g for 8 minutes to collect the PRP. Subsequently, a filtration process was employed to remove WBCs using leukocyte filtration filters. A PRP platelet count of 1 million/μL has been identified as the optimal therapeutic dose [17]. The PRP was divided into aliquots and stored at −20 °C for subsequent use [19,20].

4. Blood sampling and hormone assay

To measure the levels of T3, T4, and testosterone, blood samples were collected via cardiac puncture and subsequently centrifuged at 3,500 rpm for 15 minutes. Following centrifugation, serum samples were stored at −70 °C for further biochemical analysis [21,22]. The concentrations of T3, T4, and testosterone were determined using an enzyme-linked immunosorbent assay kit (Monobind Inc.).

5. Spermatozoa collection and assessment

To obtain a sperm suspension, the caudal portion of the epididymis was excised and minced in a Petri dish containing 2 mL of physiological saline (0.9% NaCl) at 37 °C for 5 to 10 minutes [23]. To evaluate the sperm count, we manually counted the sperm heads by examining the samples under a light microscope using a Neubauer hemocytometer. We counted between 200 and 300 spermatozoa for each rat [24].

To assess sperm motility, microscope slides were preheated on a heating table set to 37 °C before the sperm suspension was applied to each slide. The slides were then randomly examined across 10 microscopic fields, with 200 to 300 spermatozoa assessed per animal. Sperm motility was categorized as progressive, non-progressive, or immotile. Progressive motility was characterized by spermatozoa moving in a straight line, non-progressive motility was indicated by spermatozoa moving in a circular pattern, and immotile spermatozoa exhibited no movement whatsoever [13].

https://doi.org/10.5653/cerm.2023.06695

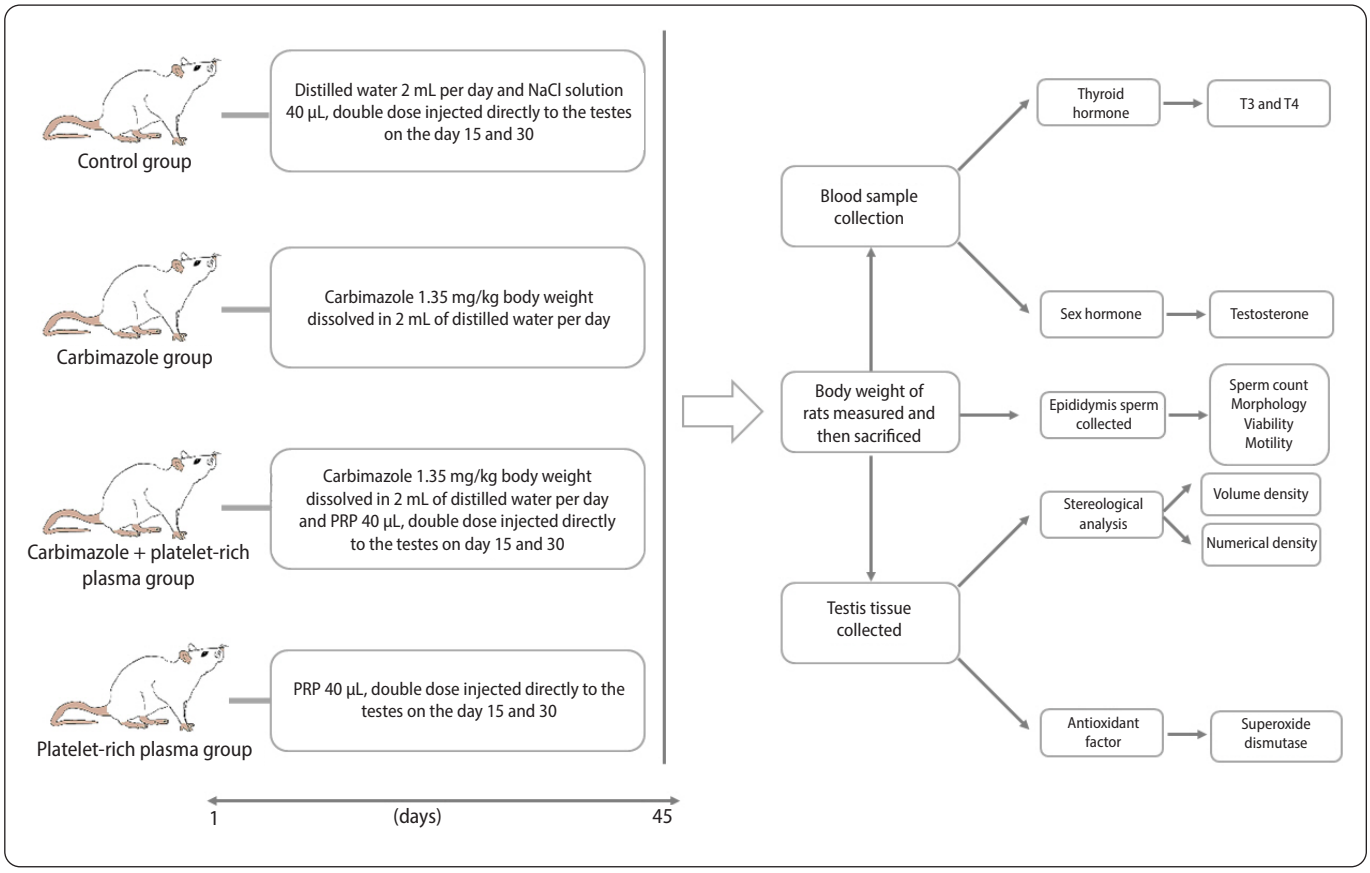

Figure 1. Schematic representation of the experimental design, showing the study groups and the timeline. PRP, platelet-rich plasma; T3, triiodothyronine; T4, thyroxine.

Sperm viability was assessed using eosin Y staining. A 10-µL volume of each sample was mixed with an equal volume of eosin Y solution. Subsequently, the samples were smeared on slides and allowed to air-dry for 5 to 10 minutes. We examined over 200 spermatozoa under a light microscope. Sperm that remained unstained were considered living, while those that took up the pink or red (eosin) stain were identified as dead [17].

To analyze sperm morphology, a suspension of sperm was placed on a microscope slide. The smear was subsequently air-dried and stained with 1% eosin Y for 5 to 10 minutes. For each rat, between 200 and 300 spermatozoa were examined, and the ratio of normal to abnormal spermatozoa was determined. Abnormal sperm morphology was defined as the presence of any irregularities in the head or tail [21].

6. Stereological study

On the final day of the experiment, the left testis was excised, and its weight was recorded. Subsequently, its primary volume, denoted as V (testis), was determined using the immersion method. For stereological analysis, the left testis was preserved in a 4% buffered formaldehyde solution. Following the orientator method, isotropic uniform random sections were prepared. This technique yielded approximately eight to 12 slabs from each testis. To assess tissue shrinkage, a circular piece was excised from a randomly selected testis slab using a trocar with a 4-mm diameter. After tissue processing, the circular piece and slabs were embedded, sectioned at respective thicknesses of 5 and 25 µm, and stained with hematoxylin and eosin (Figure 2). The areas of the circular pieces were measured both before processing (the unshrunken state) and after (the shrunken state) [21,25]. The degree of shrinkage, represented as d (shr), was then calculated using the following formula:

$$d\,(shr)=1-[Area\,(after)/Area\,(before)]^{1.5}$$

The total volume of the testis was measured based on shrinkage volume (V [shrunken]), calculated using the following formula:

$$V\,(shrunken)=V\,(unshrunken)\times[1-d\,(shr)]$$

7. Estimation of the volumes of testicular components

The volume densities of the seminiferous tubules, germinal epithelium, lumen of each tubule, and interstitial tissue were estimated using the point-counting method. A point grid was overlaid on the

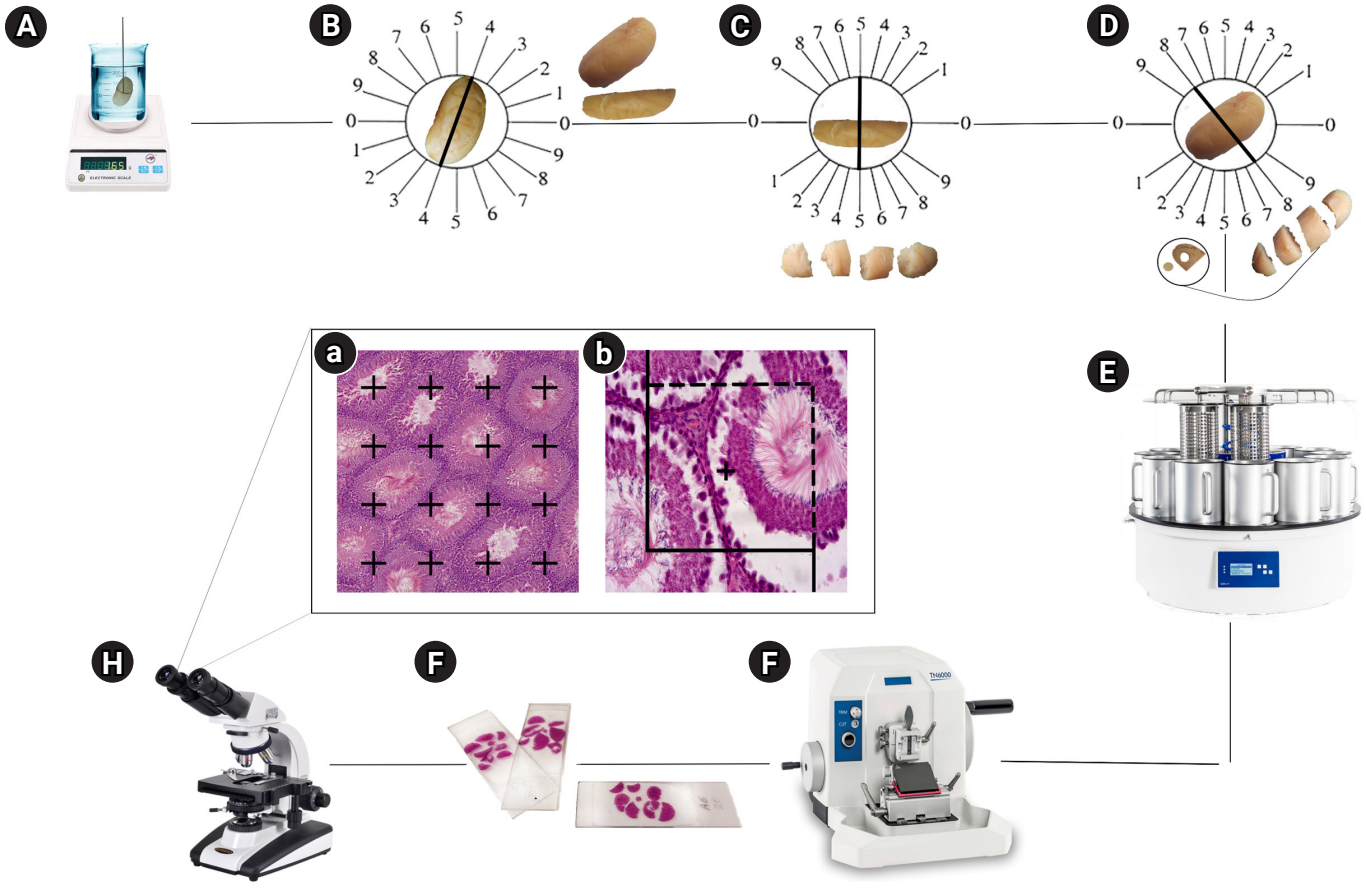

Figure 2. Stereological techniques for quantitative analysis. (A) Testicular volume was assessed using the immersion method. (B) Uniform isotropic tissue sections were prepared in accordance with the orientator method. The testis was divided into halves along a randomly selected direction within the evenly divided circle. (C, D) Each half was then cut in a random direction from the cosine-weighted divided circle, resulting in 8–10 slabs collected from each testis. A circle was punched out from a random slice. (E, F, G) Tissue processing, sectioning, and slide preparation were performed. (Ha) Finally, the point-counting method was used to assess the volume density of the structures, and (Hb) optical sections of the testicular tissue were examined to determine the numerical densities of various cells (H&E staining, ×400 magnification).

live microscopic image of the sections, which had a thickness of 5 μm, during monitoring. This was achieved using software developed at the Centre of Histomorphometry and Stereology [21,26].

The volume density, denoted as "Vv (structure/testis)," of each structure was calculated using the following formula:

$$Vv\ (structure/testis) = \Sigma P\ (structure) / \Sigma P\ (testis)$$

Here, ∑P (structure) refers to the number of points intersecting the profiles of the seminiferous tubules, germinal epithelium, the lumen of each tubule, and the interstitial tissue. ΣP (testis) denotes the number of points intersecting the testis.

The total, or absolute, volume of each component was determined by multiplying its volume density by the final volume of the testis:

$$V\ (structure) = Vv\ (structure/testis) \times V\ (shrunken)$$

8. Estimation of the number of testicular cells of various types

The total numbers of testicular cells of several types—including spermatogonia, spermatocytes, round and elongated spermatids, Sertoli cells, and Leydig cells—were estimated using the optical disector method. This technique was applied to hematoxylin and eosin-stained sections that were 25 μm thick, utilizing a computer-assisted light microscope (E200; Nikon) equipped with a ×40 oil immersion lens. Subsequently, microscopic fields were examined through systematic uniform random sampling, which involved moving the microscope stage at equal intervals in the X and Y directions. Adjustments in the Z direction were made using a microcator (MT12; Heidenhain) fixed on the microscope stage. The distribution of testicular cells across different focal planes in the Z-axis was analyzed to determine the disector's height and the guard zones [13,21,27]. To

https://doi.org/10.5653/cerm.2023.06695

estimate the numerical density—termed "Nv (cells/testicle)" and representing the number of cells per unit volume of the germinal epithelium—the following formula was employed:

$$Nv\ (cells/testis)=\Sigma Q/(\Sigma A\times h)\times(t/BA)$$

The total number of nuclei from each cell type that came into focus was represented by ΣQ, with ΣA denoting the total area of the unbiased counting frame, h representing the height of the disector, t indicating the mean section thickness, and BA reflecting the advance of the microtome block. Ultimately, to determine the total number of testicular cells by type, the numerical density (Nv) was multiplied by the volume of the structure (V):

$$N\ (cells)=Nv\times V\ (structure)$$

Here, V (structure) represented the total volume of interstitial tissue for the Leydig cells and the total volume of germinal epithelium for the germinal layer cells.

9. Determination of antioxidant levels via superoxide dismutase assay

Superoxide dismutases (SODs) catalyze the dismutation of the superoxide anion free radical (O_2–) into molecular oxygen and hydrogen peroxide (H_2O_2). This reaction is crucial for the regulation of the antioxidant defense system. To assess SOD activity, we followed the protocol established by Pal and Mukhopadhyay [28]. Testicular tissue was homogenized in 1 mL of phosphate buffer (pH 7.4) and then centrifuged at 10,000 ×g for 10 minutes at 4 °C. The supernatant was collected, transferred to fresh tubes, and placed on ice. Samples designated for biochemical assays were stored at −70 °C until use.

10. Statistical analysis

For data that met the criteria for homogeneity of variance and normality of distribution, statistical analysis was conducted using one-way analysis of variance (ANOVA). Outcomes are presented as mean±standard deviation to represent the range of possible results across groups. The Tukey test was utilized for *post hoc* comparisons following ANOVA. *p*-values of less than 0.05 were considered to indicate statistical significance. For data that did not follow a normal distribution, the Kruskal-Wallis test was used. All statistical analyses were carried out with Graph Pad Prism ver. 5 (GraphPad Software Inc.).

Results

1. Body weight

After 45 days, we observed no statistically significant changes in body weight among the various treatment groups (Table 1).

2. Testis weight

The results indicated a significantly lower testicular weight in the CBZ group compared with the control rats ($p<0.0001$). The reduction in testicular weight was less pronounced in the CBZ+PRP animals relative to the CBZ group ($p<0.01$) (Table 1).

3. Testicular volume

The testicular volume of the CBZ group was significantly lower than that of the control animals ($p<0.0001$). However, the rats treated with CBZ+PRP exhibited a smaller decline in testicular volume than those in the CBZ group ($p<0.01$) (Figure 3).

4. Spermatozoa count, viability, morphology, and motility

Figure 4 demonstrates that, in comparison to the control rats, the sperm count, viability, normal morphology, and progressive and non-progressive motility were dramatically lower in the CBZ group ($p<0.0001$). When compared to the control group, the percentage of immotile sperm was significantly higher in the CBZ group ($p<0.0001$). Additionally, PRP therapy in the CBZ+PRP group enhanced sperm count, vitality, normal morphology, progressive and non-progressive motility, while decreasing the percentages of immotile sperm, relative to the CBZ group ($p<0.0001$).

Table 1. Comparison of body weight, testis weight, levels of serum T3, T4, testosterone hormones, and SOD parameters between the groups of the CON, CBZ, CBZ+PRP, and PRP groups (n=10)

Variable	CON	CBZ	CBZ+PRP	PRP
Body weight (g)	286.9 ± 16.62	277.4 ± 14.74	278.7 ± 12.93	291.3 ± 33.66
Testis weight (g)	1.56 ± 0.08	1.26 ± 0.03[a]	1.35 ± 0.09[b]	1.52 ± 0.09
T3 (ng/mL)	1.33 ± 0.06	0.73 ± 0.04[a]	0.78 ± 0.04	1.30 ± 0.04
T4 (ng/mL)	42.11 ± 4.20	25.63 ± 3.67[a]	25.96 ± 2.09	40.32 ± 2.87
Testosterone (ng/mL)	3.23 ± 1.03	1.03 ± 0.33[a]	2.36 ± 0.93[c]	3.10 ± 0.86
SOD (U/mg protein)	31.94 ± 3.66	11.53 ± 6.49[a]	17.65 ± 4.06[b]	33.44 ± 4.7

Values are presented as mean±standard deviation.
T3, triiodothyronine; T4, thyroxine; SOD, superoxide dismutase; CON, control; CBZ, carbimazole; PRP, platelet-rich plasma.
[a] $p<0.0001$ (CBZ vs. CON); [b] $p<0.01$, [c] $p<0.001$ (CBZ+PRP vs. CBZ).

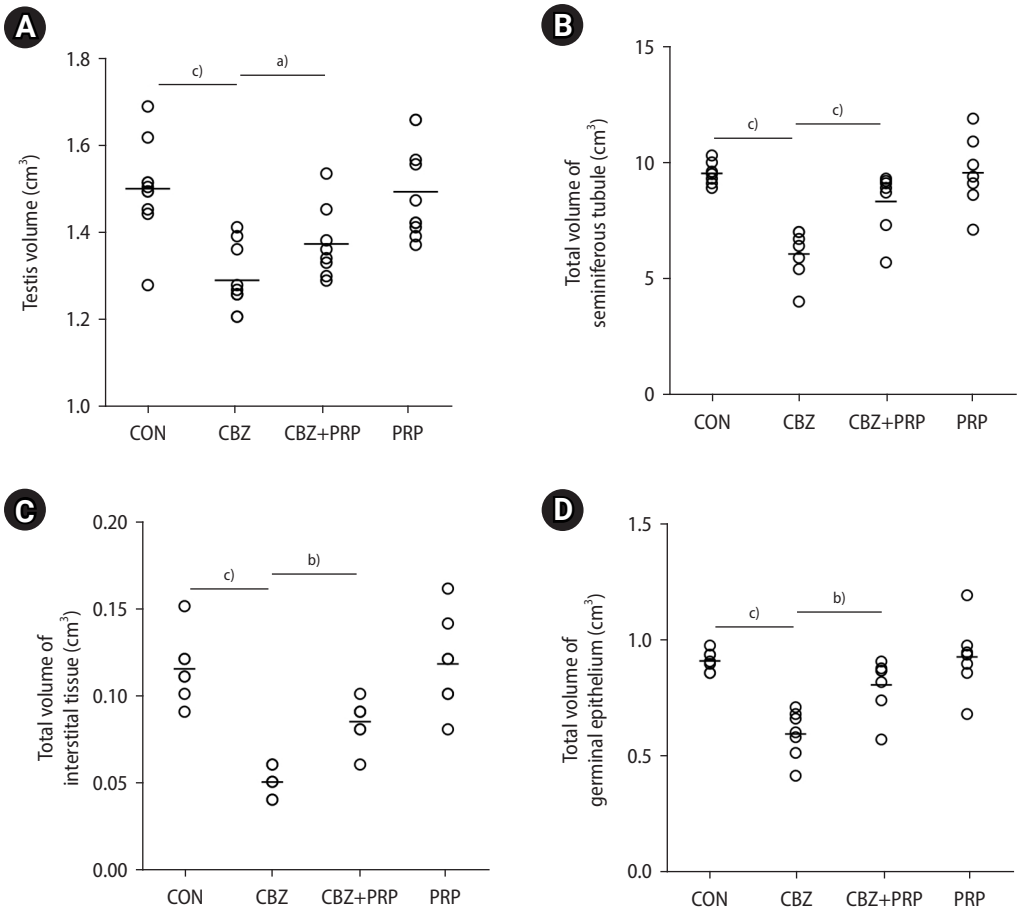

Figure 3. Dot plots illustrate the total volume of the testis and various testicular components: (A) testis, (B) seminiferous tubules, (C) interstitial tissue, and (D) germinal epithelium. These values are presented across four groups: control (CON), carbimazole (CBZ), CBZ+platelet-rich plasma (PRP), and PRP alone. The horizontal bars represent the mean values for each parameter within the groups. [a)]$p<0.01$; [b)]$p<0.001$; [c)]$p<0.0001$.

5. Serum levels of T3, T4, testosterone, and SOD activity

Serum concentrations of total T3 and T4 were significantly lower in the CBZ and CBZ+PRP groups compared to the control group ($p<0.0001$). Testosterone levels in the control, CBZ, and CBZ+PRP groups were 3.21±1.03, 1.03±0.33, and 2.36±0.92 ng/mL, respectively, indicating a statistically significant difference among the groups. The mean total testosterone level in the CBZ group was significantly lower than that in the control group ($p<0.0001$), while the mean total testosterone level in the CBZ+PRP group was significantly higher than the level in the CBZ group ($p<0.001$). Additionally, CBZ exposure significantly reduced SOD antioxidant enzyme activity in testis tissue compared with control animals ($p<0.0001$). PRP treatment resulted in significantly higher SOD activity levels in the CBZ+PRP group compared with the CBZ group ($p<0.01$). Moreover, PRP significantly restored the activity of this antioxidant enzyme in the testicular tissue (Table 1).

6. Volume of the seminiferous tubules

The tubular volumes were reduced by 36% in the rats exposed to CBZ compared to the control group ($p<0.0001$). However, this parameter showed considerable recovery in the animals that received CBZ+PRP compared to the CBZ group ($p<0.001$) (Figure 3).

7. Volume of the seminiferous tubule epithelium

The results also indicated a 34% lower total volume of the germinal epithelium in the rats treated with CBZ compared to the control animals ($p<0.0001$). However, this reduction was significantly mitigated in the CBZ+PRP group when compared to the CBZ-only group ($p<0.001$) (Figure 3).

8. Volume of the interstitial tissue

The volume of interstitial tissue was significantly lower in the CBZ group compared to the control group ($p<0.0001$). However, this re-

https://doi.org/10.5653/cerm.2023.06695

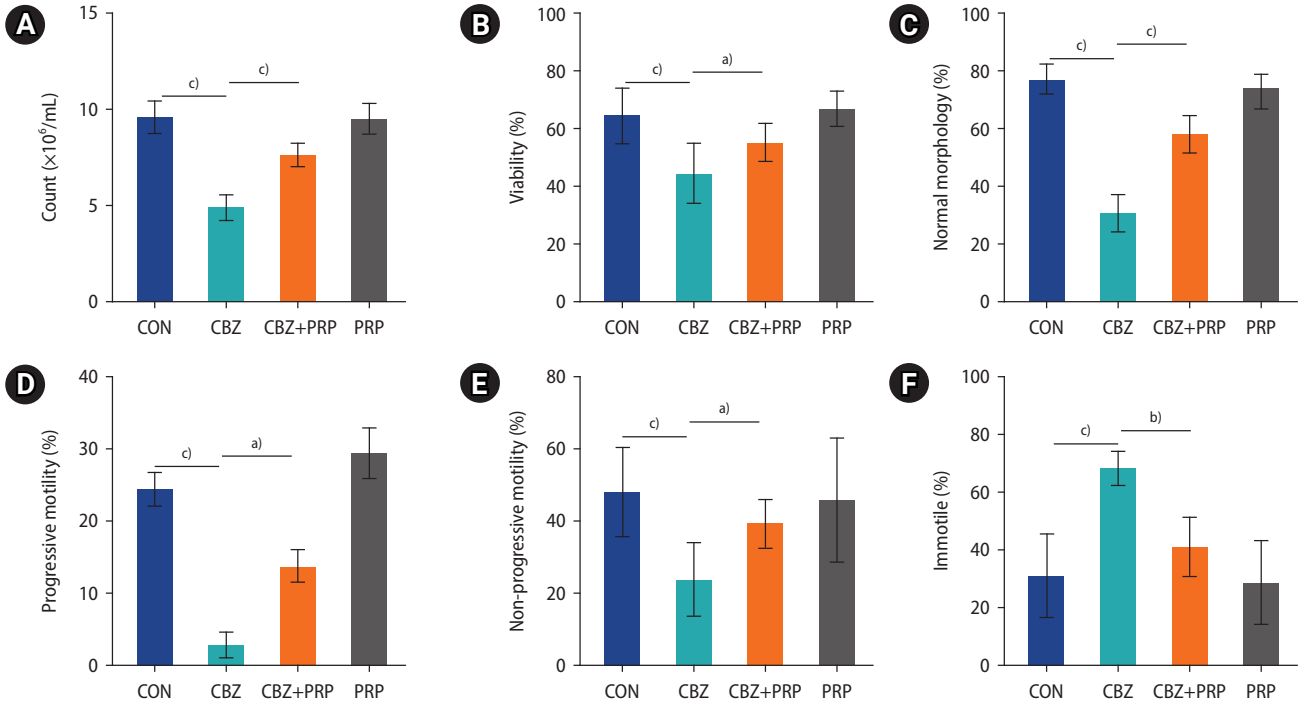

Figure 4. Comparison of (A) sperm count, (B) viability, (C) normal morphology, (D) progressive motility, (E) non-progressive motility, and (F) immotility across the control (CON), carbimazole (CBZ), CBZ+platelet-rich plasma (PRP), and PRP groups. The horizontal bars represent the mean values for each parameter within the groups. Data are expressed as mean±standard deviation, with n=10 for each group. [a)]$p<0.01$; [b)]$p<0.001$; [c)]$p<0.0001$.

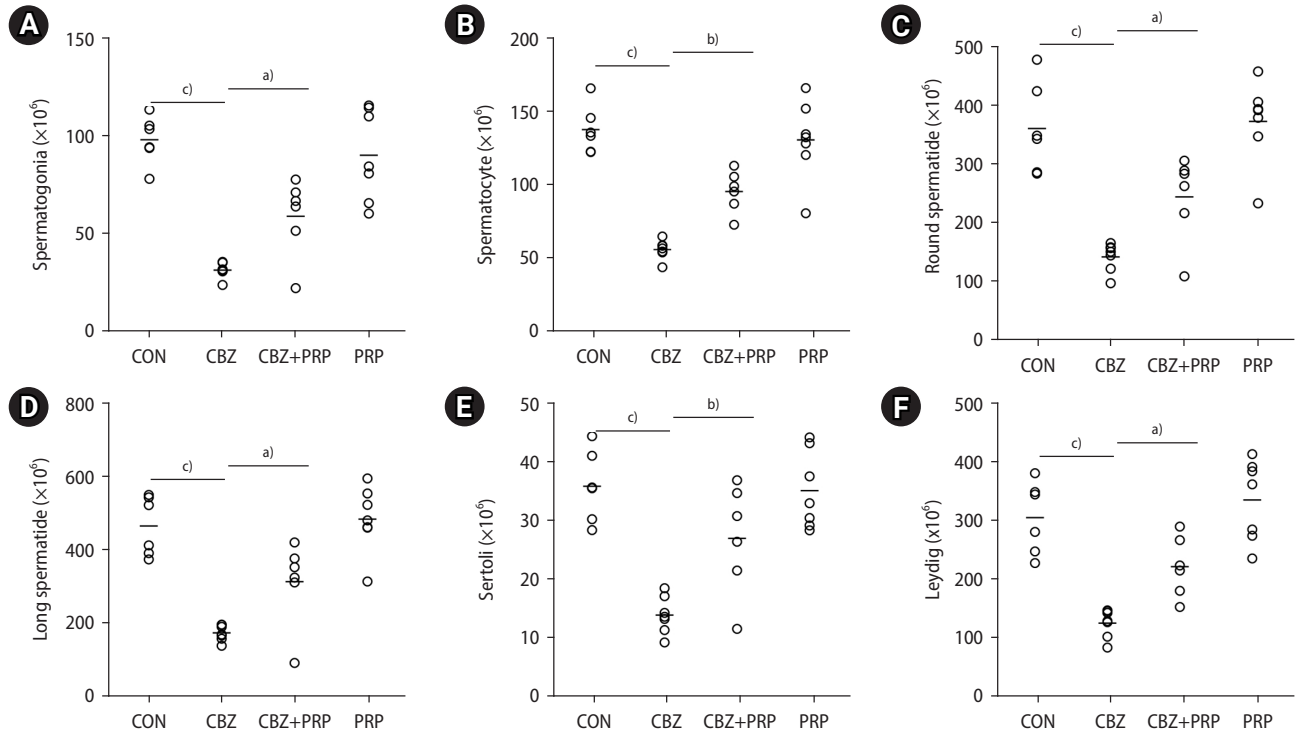

Figure 5. Dot plots indicate the total counts of (A) spermatogonia, (B) spermatocytes, (C) round spermatids, (D) elongated spermatids, (E) Sertoli cells, and (F) Leydig cells across four groups: control (CON), carbimazole (CBZ), CBZ+platelet-rich plasma (PRP), and PRP alone. The horizontal bars represent the mean values for each parameter within the groups. [a)]$p<0.01$; [b)]$p<0.001$; [c)]$p<0.0001$.

duction was mitigated in the CBZ+PRP animals (p<0.001) (Figure 3).

9. Number of cells by type

The total numbers of testicular cells of various types (spermatogonia, spermatocytes, round spermatids, elongated spermatids, Sertoli cells, and Leydig cells) decreased by 68%, 59%, 60%, 58%, 67%, and 59%, respectively, in the CBZ group compared to the control group (p<0.0001). The counts of spermatogonia, spermatocytes, round and elongated spermatids, Sertoli cells, and Leydig cells were significantly higher in the CBZ+PRP group than in the CBZ group alone (p<0.0001) (Figure 5).

10. Qualitative changes

The qualitative evaluation of the testis is illustrated in Figure 6. Histological analysis of rats treated with CBZ revealed marked structural changes, including atrophy and a reduced number of seminiferous tubules. However, the co-administration of PRP with CBZ mitigated these adverse effects.

Discussion

The first part of our study highlights the detrimental effects of HT on sperm parameters and structural changes in the testes. Consistent with our results, Cooke et al. [29] observed a decrease in sperm count in cases of neonatal HT, which they attributed to increased apoptosis and cell death. Similarly, research has indicated that HT can lead to reduced sperm count and motility in the epididymis of rats exposed to CBZ [30]. Our findings also indicated that testicular structural changes, including reduced volume of the testis, seminiferous tubules, germinal epithelium, and interstitial tissue, could stem from testicular abnormalities and tubular atrophy associated with HT. The observed decline in sperm quality and quantity may be due to disruptions in spermatogenic cells, as seen in HT-affected rats. In 2020, Ibrahim et al. [18] found that CBZ exposure could decrease sperm count by reducing spermatocyte density and germinal epithelium thickness. Another cell type present in the tubules is the Sertoli cell, which provides nutritional and structural support [31]. The loss of these cells in HT-treated rats may lead to declines in supportive functions and spermatogenic cells. A reduction in the volume of testicular structures may be largely attributable to a decreased number of Sertoli cells, as reported by Lara et al. [32]. It has been hypothesized that a reduction in Sertoli and Leydig cell numbers could lead to a decrease in germ cells [13]. The decline in Sertoli cells following HT may be linked to lower testosterone levels. Moreover, we observed decreases in both Leydig cell numbers and testosterone levels. Fadlalla et al. [4] also noted a reduction in Leydig cell numbers in HT groups. Additionally, HT is known to promote oxidative stress,

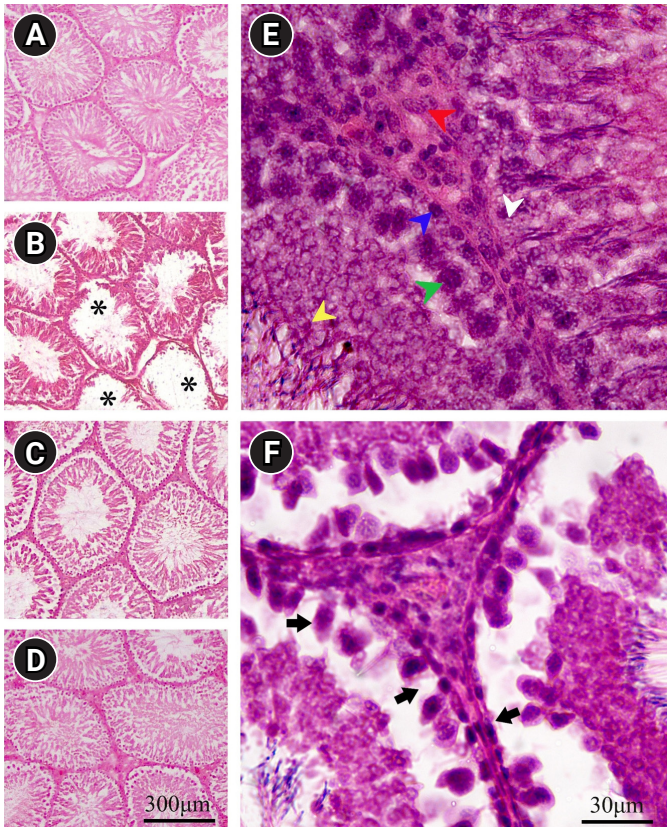

Figure 6. Microscopic evaluation of testicular tissue in the (A) control (CON), (B) carbimazole (CBZ), (C) CBZ+platelet-rich plasma (PRP), and (D) PRP groups. The spermatogenic cells, including spermatogonia (blue arrow), spermatocytes (green arrow), spermatids (yellow arrow), Sertoli cells (white arrow), and Leydig cells (red arrow), are depicted in the (E) CON group. Image (B) shows that the germinal epithelium of the seminiferous tubules has degenerated (asterisks). (F) A reduction in germ cells, small spermatogonia with dark nuclei, and disarrangement of spermatocytes throughout the lumen of the seminiferous tubule are evident in the CBZ group (arrows). (C) Concurrent treatment of the hypothyroidism-affected rats with PRP increased the numbers of various testicular cell types. Scale bar=300 μm in images (A, B, C, D) and 30 μm in images (E, F), H&E staining.

which exacerbates the condition by inhibiting deiodinases and establishing a vicious circle [33]. In line with this, we observed a significant decrease in SOD antioxidant activity in the testes of HT rats. This finding aligns with the research of Wang et al. [34] and Algaidi et al. [35], which indicated that HT is associated with a weakened antioxidant defense mechanism against free radicals produced during normal cellular metabolism. Studies have highlighted the importance of mitochondrial reactive oxygen species level during spermatogenesis in HT rats, as it affects both the quality and quantity of sperm, particularly in mitochondria-rich cells [36]. Research suggests that growth factors play a role in stimulating spermatogenesis and inhibiting

https://doi.org/10.5653/cerm.2023.06695

apoptosis [17,37].

Our second step reveals that treating HT animals with PRP injections significantly restored sperm parameters and mitigated testicular changes. Findings by Bader et al. [17] and Dehghani et al. [13] also indicated that PRP positively influences sperm parameters, improving sperm count, motility, and morphology. Furthermore, an earlier study reported that intratesticular injection of autologous PRP effectively enhances the function of rabbit sperm [38]. Research has demonstrated that the interaction of growth factors is crucial in regulating germ cell division, ensuring an appropriate balance between the proliferation and differentiation of germ cells [39]. Growth factors present in PRP, such as PDGF and VEGF, exert multiple effects on testicular tissue. Specifically, VEGF and its receptors play a role in testicular growth regulation, and VEGF contributes to the activation of nuclear factor erythroid 2-related factor 2, which in turn helps reduce oxidative stress during spermatogenesis [13]. Our findings corroborate the role of reproductive hormones and the reduction of oxidative stress in the beneficial effects of PRP on HT-induced testicular toxicity in rats. According to results from Kutluhan et al. [14], intratesticular PRP injections favorably impact Leydig cell proliferation and testicular steroidogenesis. One limitation of the present study was the lack of investigation into the correlation between signaling mechanisms and the restorative effect of PRP on the reproductive hormones of the hypothalamic-pituitary-gonadal axis following HT exposure.

In conclusion, based on the data obtained, the present study demonstrates that HT adversely affects sperm parameters, the volumes of testicular structures, and the number of cells in the rat spermatogenesis line. Additionally, this disorder induces oxidative stress and reduces antioxidant activity, including that of SOD, which negatively impacts the testicles. Conversely, the findings indicate the beneficial effect of intratesticular PRP injection in improving testicular parameters, the volumes of seminiferous tubules and interstitial tissue, and the number of germ cells in HT-affected rats. Therefore, it can be proposed as a potential treatment for patients with infertility due to HT.

Conflict of interest

No potential conflict of interest relevant to this article was reported.

Acknowledgments

This article was part of the dissertation written by Masoud Sattar-Shamsabadi, M.Sc., a student of anatomy. The authors would like to express their gratitude to Dr. Nasrin Shokrpour at the Research Consultation Center (RCC) for her invaluable assistance in editing this manuscript.

ORCID

Hossein Bordbar https://orcid.org/0000-0003-0363-9523
Fatemeh Karimi https://orcid.org/0000-0001-6805-277X

Author contributions

Conceptualization: HB, MSS, FD, FK. Methodology: HB, FD. Formal analysis: MSS, FK. Data curation: MSS, FK. Funding acquisition: HB, FD. Project administration: HB, FK. Visualization: HB, MSS, FD, FK. Software: MSS, FK. Validation: HB, FD, FK. Investigation: HB, FK. Writing-original draft: HB, FK. Writing-review & editing: HB, FD, FK. Approval of final manuscript: HB, MSS, FD, FK.

References

1. Mintziori G, Duntas LH, Veneti S, Goulis DG. Metabolic, oxidative and psychological stress as mediators of the effect of COVID-19 on male infertility: a literature review. Int J Environ Res Public Health 2022;19:5277.
2. Singh R, Hamada AJ, Agarwal A. Thyroid hormones in male reproduction and fertility. Open Reprod Sci J 2011;3:98-104.
3. Unnikrishnan AG, Menon UV. Thyroid disorders in India: an epidemiological perspective. Indian J Endocrinol Metab 2011;15:S78-81.
4. Fadlalla MB, Wei Q, Fedail JS, Mehfooz A, Mao D, Shi F. Effects of hyper- and hypothyroidism on the development and proliferation of testicular cells in prepubertal rats. Anim Sci J 2017;88:1943-54.
5. Nascimento Gomes S, do Carmo Correa DE, de Oliveira IM, Bargi-Souza P, Degraf Cavallin M, Dobner Mariano D, et al. Imbalanced testicular metabolism induced by thyroid disorders: new evidences from quantitative proteome. Endocrine 2020;67:209-23.
6. Jalilvand N, Hosseini M, Beheshti F, Ebrahimzadeh-Bideskan A. Protective effect of PPARγ agonist pioglitazone, on testicular tissue and sperm parameters in hypothyroid rats. Toxin Rev 2021;40:267-76.
7. Amra EA, El Rehim SAA, Lashein FM, Shoaeb HS. Effect of a bradykinin potentiating factor separated from honey bee venom on thyroid gland and testis in hypothyroid white rats. J Basic Appl Zool 2022;83:1.
8. Arafa MA, Gouda ZA, El-Naseery NI, Abdel-Nour HM, Hanafy SM, Mohamed AF, et al. Bone marrow-derived mesenchymal stem cells ameliorate the pancreatic changes of chemically induced hypothyroidism by carbimazole in male rats. Cells Tissues Organs

2018;206:144-56.
9. La Vignera S, Vita R, Condorelli RA, Mongioi LM, Presti S, Benvenga S, et al. Impact of thyroid disease on testicular function. Endocrine 2017;58:397-407.
10. Nikoobakht MR, Aloosh M, Nikoobakht N, Mehrsay AR, Biniaz F, Karjalian MA. The role of hypothyroidism in male infertility and erectile dysfunction. Urol J 2012;9:405-9.
11. Negro R, Greco G. Levothyroxine but not selenium increases endothelial progenitor cell counts in patients with hypothyroidism. Eur Thyroid J 2016;5:100-5.
12. Chakrabarti SK, Ghosh S, Banerjee S, Mukherjee S, Chowdhury S. Oxidative stress in hypothyroid patients and the role of antioxidant supplementation. Indian J Endocrinol Metab 2016;20:674-8.
13. Dehghani F, Sotoude N, Bordbar H, Panjeshahin MR, Karbalay-Doust S. The use of platelet-rich plasma (PRP) to improve structural impairment of rat testis induced by busulfan. Platelets 2019;30:513-20.
14. Kutluhan MA, Ozsoy E, Sahin A, Urkmez A, Topaktas R, Toprak T, et al. Effects of platelet-rich plasma on spermatogenesis and hormone production in an experimental testicular torsion model. Andrology 2021;9:407-13.
15. Sekerci CA, Tanidir Y, Sener TE, Sener G, Cevik O, Yarat A, et al. Effects of platelet-rich plasma against experimental ischemia/reperfusion injury in rat testis. J Pediatr Urol 2017;13:317.
16. Sharara FI, Lelea LL, Rahman S, Klebanoff JS, Moawad GN. A narrative review of platelet-rich plasma (PRP) in reproductive medicine. J Assist Reprod Genet 2021;38:1003-12.
17. Bader R, Ibrahim JN, Moussa M, Mourad A, Azoury J, Azoury J, et al. In vitro effect of autologous platelet-rich plasma on H2 O2-induced oxidative stress in human spermatozoa. Andrology 2020;8:191-200.
18. Ibrahim AA, Mohammed NA, Eid KA, Abomughaid MM, Abdelazim AM, Aboregela AM. Hypothyroidism: morphological and metabolic changes in the testis of adult albino rat and the amelioration by alpha-lipoic acid. Folia Morphol (Warsz) 2021;80:352-62.
19. Dehghani F, Hassanpour A, Poost-Pasand A, Noorafshan A, Karbalay-Doust S. Protective effects of L-carnitine and homogenized testis tissue on the testis and sperm parameters of busulfan-induced infertile male rats. Iran J Reprod Med 2013;11:693-704.
20. Bordbar H, Esmaeilpour T, Dehghani F, Panjehshahin MR. Stereological study of the effect of ginger's alcoholic extract on the testis in busulfan-induced infertility in rats. Iran J Reprod Med 2013;11:467-72.
21. Bordbar H, Yahyavi SS, Noorafshan A, Aliabadi E, Naseh M. Resveratrol ameliorates bisphenol A-induced testicular toxicity in adult male rats: a stereological and functional study. Basic Clin Androl 2023;33:1.
22. Kar A, Panda S, Singh M, Biswas S. Regulation of PTU-induced hypothyroidism in rats by caffeic acid primarily by activating thyrotropin receptors and by inhibiting oxidative stress. Phytomed Plus 2022;2:100298.
23. Prathima P, Venkaiah K, Pavani R, Daveedu T, Munikumar M, Gobinath M, et al. α-Lipoic acid inhibits oxidative stress in testis and attenuates testicular toxicity in rats exposed to carbimazole during embryonic period. Toxicol Rep 2017;4:373-81.
24. Aminsharifi A, Hekmati P, Noorafshan A, Karbalay-Doost S, Nadimi E, Aryafar A, et al. Scrotal cooling to protect against cisplatin-induced spermatogenesis toxicity: preliminary outcome of an experimental controlled trial. Urology 2016;91:90-8.
25. Karimi F, Noorafshan A, Karbalay-Doust S, Naseh M. Sleep deprivation induces structural changes in the adult rat testis: the protective effects of olive oil. Clin Exp Reprod Med 2023;50:19-25.
26. Tschanz S, Schneider JP, Knudsen L. Design-based stereology: planning, volumetry and sampling are crucial steps for a successful study. Ann Anat 2014;196:3-11.
27. von Bartheld CS. Distribution of particles in the Z-axis of tissue sections: relevance for counting methods. Neuroquantology 2012;10:66-75.
28. Pal P, Mukhopadhyay PK. Fluoride induced testicular toxicities in adult Wistar rats. Toxicol Mech Methods 2021;31:383-92.
29. Cooke PS, Zhao YD, Hansen LG. Neonatal polychlorinated biphenyl treatment increases adult testis size and sperm production in the rat. Toxicol Appl Pharmacol 1996;136:112-7.
30. Francois Xavier KN, Patrick Brice DD, Modeste WN, Esther N, Albert K, Pierre K, et al. Preventive effects of Aframomum melegueta extracts on the reproductive complications of propylthiouracil-induced hypothyroidism in male rat. Andrologia 2019;51:e13306.
31. Ni FD, Hao SL, Yang WX. Multiple signaling pathways in Sertoli cells: recent findings in spermatogenesis. Cell Death Dis 2019;10:541.
32. Lara NL, Silva VA, Chiarini-Garcia H, Garcia SK, Debeljuk L, Hess RA, et al. Hypothyroidism induced by postnatal PTU (6-n-propyl-2-thiouracil) treatment decreases Sertoli cell number and spermatogenic efficiency in sexually mature pigs. Gen Comp Endocrinol 2020;299:113593.
33. Mancini D, Dameri RP, Bonollo E. Looking for synergies between accounting and information technologies. In: Mancini D, Dameri RP, Bonollo E, editors. Strengthening information and control systems: the synergy between information technology and accounting models. Springer; 2016. p. 1-12.
34. Wang Q, Hong W, Chen S, Zhang Q. Variation with semilunar periodicity of plasma steroid hormone production in the mudskipper Boleophthalmus pectinirostris. Gen Comp Endocrinol 2008;155:821-6.
35. Algaidi SA, Faddladdeen KA, Alrefaei GI, Qahl SH, Albadawi EA, ALmohaimeed HM, et al. Thymoquinone protects the testes of hypothyroid rats by suppressing pro-inflammatory cytokines and oxidative stress and promoting SIRT1 testicular expression. Front Pharmacol 2022;13:1040857.

https://doi.org/10.5653/cerm.2023.06695

36. Divakaruni AS, Wiley SE, Rogers GW, Andreyev AY, Petrosyan S, Loviscach M, et al. Thiazolidinediones are acute, specific inhibitors of the mitochondrial pyruvate carrier. Proc Natl Acad Sci U S A 2013;110:5422-7.
37. Farbman AI, Buchholz JA. Transforming growth factor-alpha and other growth factors stimulate cell division in olfactory epithelium in vitro. J Neurobiol 1996;30:267-80.
38. Abdulla AK, Rebai T, Al-Delemi DH. Protective effects of autologous platelet-rich plasma (PRP) on the outcome of cryopreservation in rabbit sperm. Cell Mol Biol (Noisy-le-grand) 2022;68:113-21.
39. Feng CW, Bowles J, Koopman P. Control of mammalian germ cell entry into meiosis. Mol Cell Endocrinol 2014;382:488-97.